Journal Pre-proof

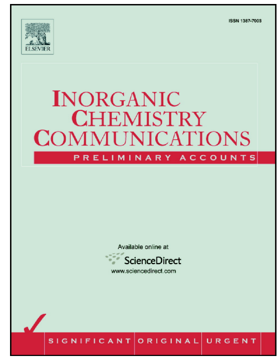

High-performance supercapacitors and non-enzymatic electrochemical glucose sensor based on tremella-like NiS/CoS/NiCo2S4 hierarchical structure

Danqing Li, Xia Zhang, Lei Pei, Chaoyang Dong, Jianguo Shi, Yuandong Xu

PII: S1387-7003(19)30742-7

DOI: https://doi.org/10.1016/j.inoche.2019.107581

Reference: INOCHE 107581

To appear in: *Inorganic Chemistry Communications*

Received date: 22 July 2019

Revised date: 11 September 2019

Accepted date: 12 September 2019

Please cite this article as: D. Li, X. Zhang, L. Pei, et al., High-performance supercapacitors and non-enzymatic electrochemical glucose sensor based on tremella-like NiS/CoS/NiCo2S4 hierarchical structure, *Inorganic Chemistry Communications* (2018), https://doi.org/10.1016/j.inoche.2019.107581

High-performance supercapacitors and non-enzymatic electrochemical glucose sensor based on tremella-like $NiS/CoS/NiCo_2S_4$ hierarchical structure

Danqing Li, Xia Zhang*, Lei Pei, Chaoyang Dong, Jianguo Shi, Yuandong Xu*

School of Chemistry and Chemical Engineering, Henan University of Technology, Zhengzhou 450001, PR China

Abstract

$NiS/CoS/NiCo_2S_4$ microflower with hierarchical structure is successfully prepared via facile hydrothermal method. The supercapacitive performance displays that the specific capacitance is up to 513 F g^{-1} at a scan rate of 1 mV s^{-1}. The obvious redox peaks on the cyclic voltammetry curves reveal pseudocapacitive performance of $NiS/CoS/NiCo_2S_4$. Furthermore, the glucose detection behavior of $NiS/CoS/NiCo_2S_4$ modified electrode ($NiS/CoS/NiCo_2S_4$/GCE) has also been performed. Amperometric study indicates that this non-enzymatic sensor displays excellent electrocatalytic performance to glucose. The glucose diffusion from the solution to the electrode surface is the kinetic control process. These results indicate a potential application of $NiS/CoS/NiCo_2S_4$ for using as an electrode material in supercapacitors and glucose sensor.

Keywords: Composite materials, Hierarchical structure, Energy storage and conversion, Sensors

1. Introduction

Recently, transition metal sulfides are extensively investigated as electrodes due to its advantageous electrochemical properties. Among them, nickel and cobalt sulfides are promising electrode materials in supercapacitors because of its natural abundance and high theoretical specific capacitance [1–3]. Furthermore, they are also superior materials in electrochemical sensor field [4–6]. Due to the advantageous electrocatalytic oxidation to glucose, nickel and cobalt sulfides are potential material on non-enzymatic glucose sensor. In particular, the existed studies have displayed that binary transition metal sulfides have excellent conductivity compared to corresponding transition metal oxides, ascribing to the smaller band gap [7,8]. Moreover, compared with oxide, the electronegativity of S atom is lower than that of O atom, so that it can prevent structure decomposition caused by elongation between layers [7,9]. Therefore, S atom facilitates the electron transformation so that the electrochemical property of $NiS/CoS/NiCo_2S_4$ has been improved. However, the application of

$NiS/CoS/NiCo_2S_4$ in non-enzymatic glucose sensor is scarce. For example, Kannan group produces non-enzymatic glucose sensor based on the electrochemical deposition of $NiCo_2S_4$ on patterned platinum electrode [10]. Chen et al. prepare a novel ball-in-ball hollow $NiCo_2S_4$ sphere to detect glucose [11]. The existing reports imply that the structure and morphology have great influence on the electrochemical performance. The hierarchical structure with subunit not only can provide high specific area but also can shorten the transmission path. Here in this work, the tremella-like $NiS/CoS/NiCo_2S_4$ hierarchical structure with nanosheet subunit has been synthesized. The supercapacitive performance and the electrochemical sensing property used as nonenzymatic glucose sensor have been studied.

2. Experimental section

2.1. Materials synthesis

5 mmol $NiCl_2·6H_2O$, 10 mmol $CoCl_2·6H_2O$ and 10 mmol thioacetamide were dissolved in 30 ml absolute ethanol. After being stirred for 10 min, the mixed solution was transferred to Teflon-lined autoclave and maintained at 120°C for 12 h. After cooling naturally, the resulting precipitate was filtered and washed with distilled water and absolute ethanol. Finally, the sample was dried at 80°C.

2.2. Materials characterization

The obtained $NiS/CoS/NiCo_2S_4$ was characterized by X-ray powder diffraction (XRD) on Rigaku D/Max-3B diffractometer. The microstructure was studied by transmission electron microscopy (TEM, JEM JEOL 2100) and field emission scanning electron microscopy (FESEM, JSM-6701F).

2.3. Electrochemical measurements

Electrochemical tests were carried out on CHI660E (Chenhua, Shanghai, China) electrochemical working station. The working electrode of supercapacitor was fabricated by mixing the electroactive material, carbon black and poly(tetrafluoroethylene) at a weight ratio of 75:15:10 to form a homogeneous slurry which was coated onto the nickel foam current collector. A platinum sheet and Hg/HgO were used as the counter and reference electrodes, respectively. The electrolyte is 2 M KOH aqueous solution. In glucose detection, Ag/AgCl, platinum wire and glass carbon electrode (GCE) were used as reference, auxiliary and working electrode, respectively.

3. Results and discussion

The crystal structure of the as-prepared $NiS/CoS/NiCo_2S_4$ microflower is shown in Fig. 1a. The diffraction peaks located at 30.4°, 34.8° and 45.7° are indexed to the (100), (101) and (102) crystal planes of NiS (JCPDS card No. 02–1280) [12]. The diffraction peaks at 30.8°, 35.4°, 46.9° and 54.1° are assigned to the (100), (101), (102) and (110) planes of CoS (JCPDS card No. 65–3418) [13]. And the peaks at 31.6° and 55.2° correspond to the (311) and (440) planes of $NiCo_2S_4$ (JCPDS card No. 43–1477) [14]. Fig. 1b and c displays typical FESEM and TEM images of $NiS/CoS/NiCo_2S_4$. As shown in Fig. 1b, it exhibits uniform flower-like microsphere with the diameter of approximate 1 μm. Furthermore, the $NiS/CoS/NiCo_2S_4$ microspheres are all composed of a large amount of sheet-like subunits, presenting a hierarchical structure. This can also be supported by TEM image. It is clearly seen that the nanosheet subunit is very thin and the thickness is around 50 nm. This hierarchical structure is beneficial for the contact of active material with electrolyte ions and further enhances the electrochemical performance of $NiS/CoS/NiCo_2S_4$.

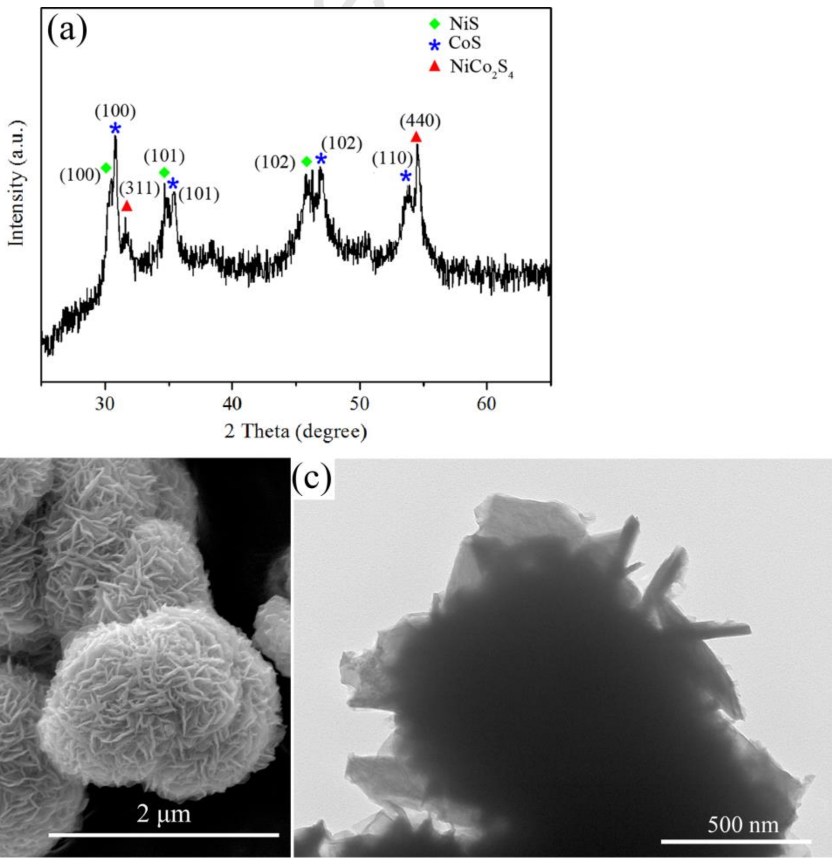

Fig. 1 (a), (b) and (c) are the XRD pattern, FESEM and TEM image of $NiS/CoS/NiCo_2S_4$, respectively.

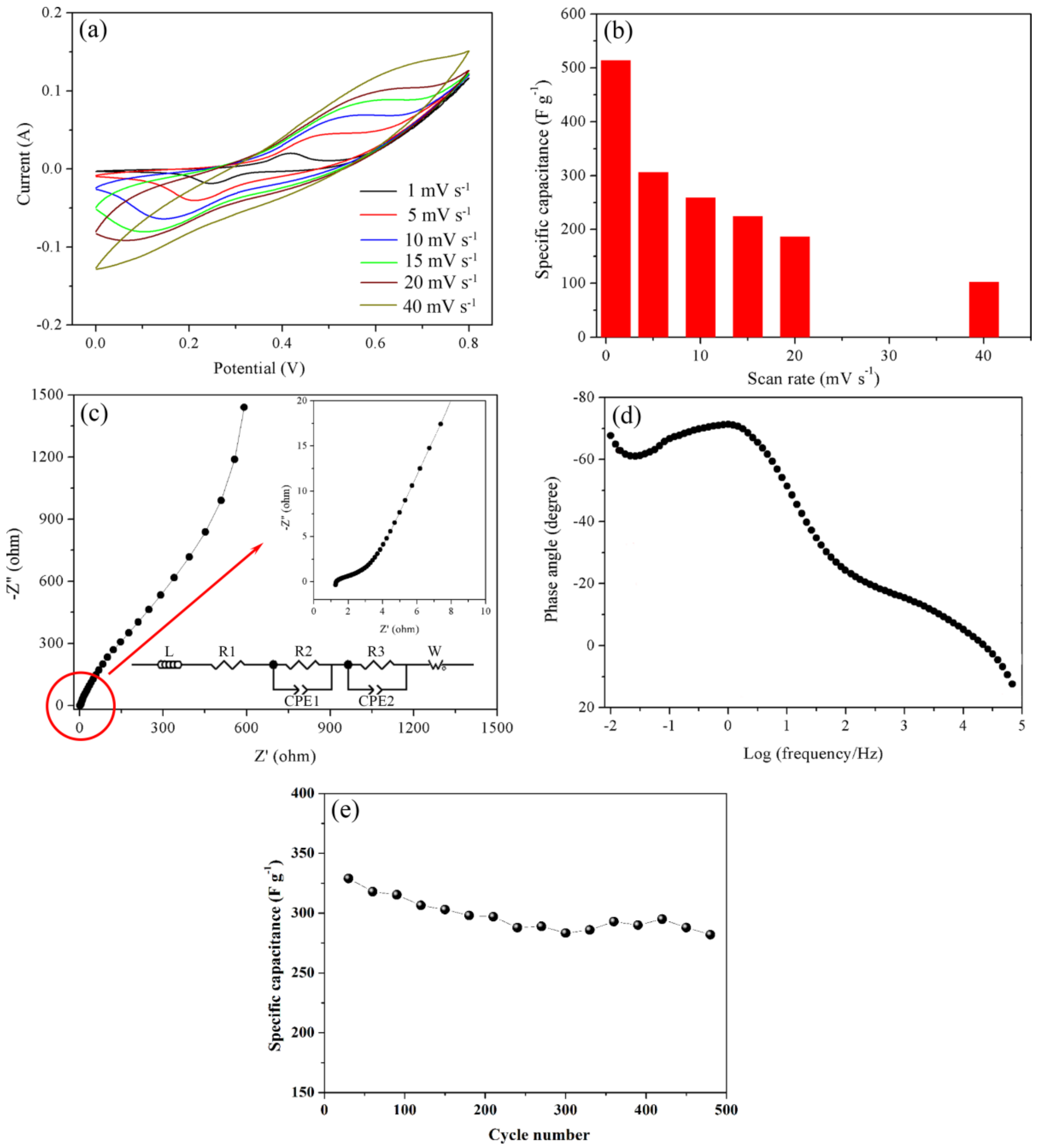

Fig. 2 (a) and (b) are CV curves and the specific capacitances of $NiS/CoS/NiCo_2S_4$ at different scan rates, (c) and (d) are the Nyquist plot and the Bode phase plot of $NiS/CoS/NiCo_2S_4$ microflower (The inset is the equivalent circuit and the enlarged area.), (e) The cycling performance of $NiS/CoS/NiCo_2S_4$ at a scan rate of 5 mV s^{-1}.

In order to investigate the supercapacitor performance of $NiS/CoS/NiCo_2S_4$ microflowers, the cyclic voltammetry (CV) tests carried out at different scan rates are shown in Fig. 2a. The CV curves exhibit obvious redox peaks at the lower scan rates (< 5 mV s^{-1}) and elliptical shape at higher scan rates (> 20 mV s^{-1}), indicating the presence of pseudocapacitive effect and the curves distortion as the scan rate increases. The reaction mechanism of $NiS/CoS/NiCo_2S_4$ in KOH solution is as follows:

$$NiS + OH^- \leftrightarrow NiSOH + e^- \qquad (1)$$

$$CoS + OH^- \leftrightarrow CoSOH + e^- \quad (2)$$

$$CoSOH + OH^- \leftrightarrow CoSO + H_2O + e^- \quad (3)$$

The specific capacitance at different scan rates for NiS/CoS/$NiCo_2S_4$ is presented in Fig. 2b. It is obvious that the values decrease with the increase of scan rates. In order to further explain the charge transfer performance of NiS/CoS/$NiCo_2S_4$, EIS measurements at a frequency range of 0.01 Hz~100 kHz is performed. The Nyquist and Bode phase plots are showed in Fig. 2c and d. The straight line in the typical Nyquist plot is the diffusive resistance of the electrolyte ions into the interior of NiS/CoS/$NiCo_2S_4$ microflowers. The two semicircles confirm the existence of two interfacial resistances which can be also reflected from the equivalent circuit (shown in the inset of Fig. 2c). The high frequency semicircle (shown in the inset) corresponds to the surface states of NiS/CoS/$NiCo_2S_4$ and the middle frequency semicircle attributes to the charge transfer resistance at the electrode/electrolyte interface [15–17]. This phenomenon can also be observed from the Bode phase plot. There are two peaks at high frequency and low frequency, respectively. The peak around 10^4 Hz corresponds to the semicircle at high frequency. Another peak around 1 Hz reflects the diffusion of electrolyte ion in the electrode solid. The cycle stability of NiS/CoS/$NiCo_2S_4$ is exhibited in Fig. 3e. At a scan rate of 5 mV s^{-1}, it presents a good cycling behavior during 500 cycles and the specific capacitance is around 300 F g^{-1}, suggesting the excellent reversibility and stability of NiS/CoS/$NiCo_2S_4$.

The sensing behavior of NiS/CoS/$NiCo_2S_4$ has also been investigated to detect glucose in NaOH electrolyte. Fig. 3a displays the CV curves of bare GCE (BGCE) and NiS/CoS/$NiCo_2S_4$/GCE. It is clear that BGCE shows no obvious redox peaks in the given potential window of 0~0.8 V, whereas NiS/CoS/$NiCo_2S_4$/GCE exhibits oxidation and reduction peaks around 0.6 V and 0.45 V, respectively. Moreover, the anodic (I_{pa}) and cathodic (I_{pc}) peak current increase distinctly in the presence of glucose, indicating that NiS/CoS/$NiCo_2S_4$/GCE exhibits prominent electrocatalytic activity toward glucose oxidation. The CV curves of NiS/CoS/$NiCo_2S_4$/GCE at different scan rates are shown in Fig. 3b. It is clear that the anodic peak (I_{pa}) shifts positively while the cathodic peak (I_{pc}) moves negatively with the increase of scan rate. As displayed in Fig. 3c, the peak current (I_p) response is linearly related to the square root of scan rate ($v^{1/2}$), manifesting that the glucose oxidation on NiS/CoS/$NiCo_2S_4$/GCE is controlled by diffusion process [18]. That is to say, the overall reaction rate of the glucose electrocatalytic oxidation is controlled by the diffusion of glucose molecules from the bulk liquid to the surface active sites of NiS/CoS/$NiCo_2S_4$ electrode.

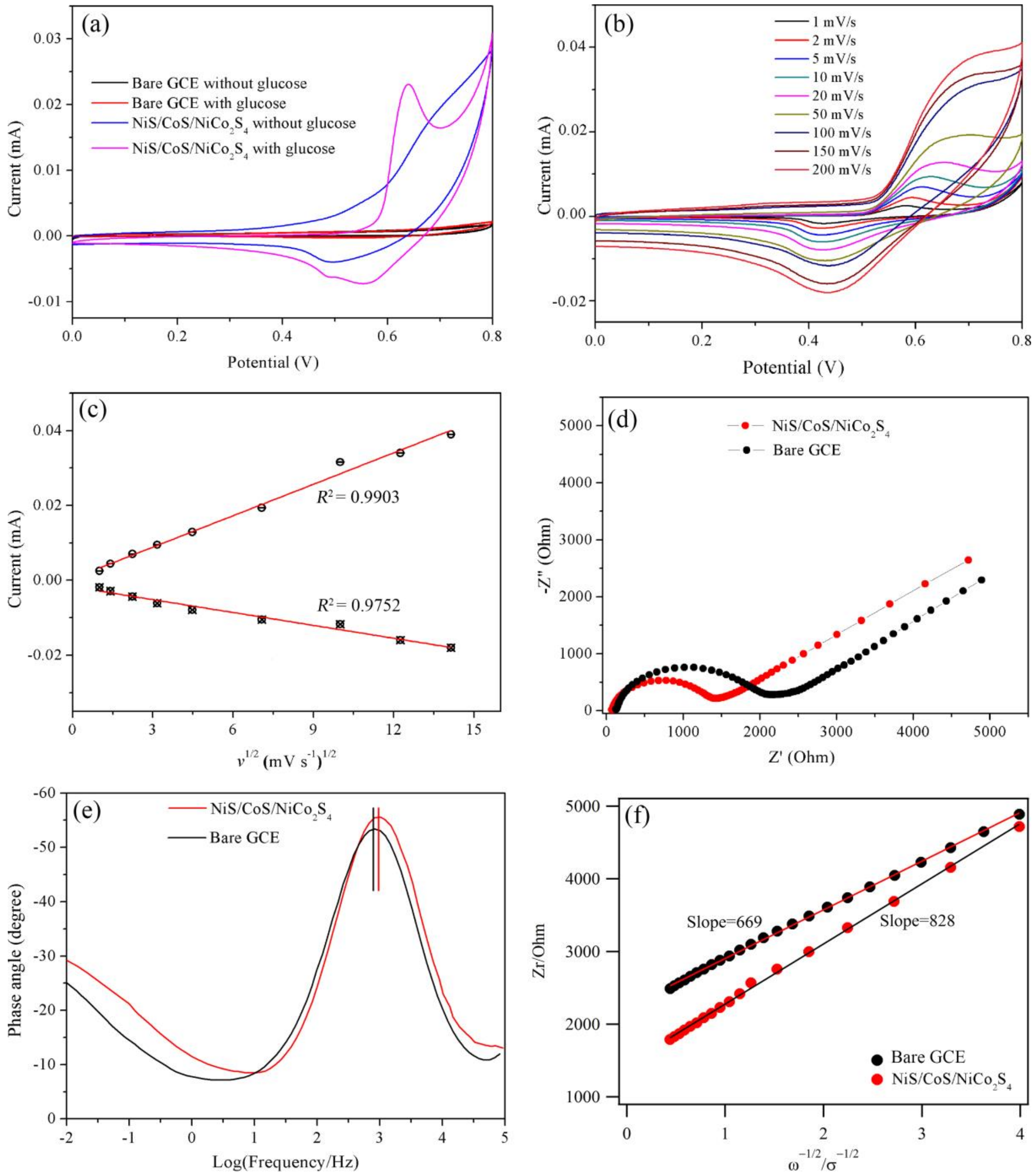

Fig. 3 (a) CV curves of GCE and NiS/CoS/$NiCo_2S_4$/GCE with or without glucose in 0.1 M NaOH at the scan rate of 50 mV s^{-1}, (b) CV curves of NiS/CoS/$NiCo_2S_4$/GCE in 0.1 M NaOH blank solution at different scan rates (1~200 mV s^{-1}), (c) Anodic and cathodic peak current vs. square root of scan rate ($v^{1/2}$), (d) Nyquist plots and (e) Phase angle Bode plots for BGCE and NiS/CoS/$NiCo_2S_4$/GCE, (f) The Z_r–$\omega^{-1/2}$ curves in the low frequency region.

To further explore the charge transfer property of $NiS/CoS/NiCo_2S_4$, EIS measurement is performed. Fig. 3d displays the Nyquist plots of BGCE and $NiS/CoS/NiCo_2S_4$/GCE in 5 mM $[Fe(CN)_6]^{3-/4-}$ with 0.1 M KCl as the supporting electrolyte. The semicircle at the high frequency region can be explained as the charge-transfer resistance (R_{ct}) corresponding to the diffusion of the electrolyte ions into the electrode through electrode/electrolyte interface [19]. The straight line corresponds to the Warburg impedance, attributing to the solid-state diffusive resistance of electrolyte ions into the interior bulk electrode. It is obvious that the radius of the semicircle for $NiS/CoS/NiCo_2S_4$/GCE is smaller than that of BGCE, suggesting the fast charge transfer speed of $NiS/CoS/NiCo_2S_4$/GCE. This result can also be supported by the Bode phase plot. As revealed in Fig. 3e, it is clear that the peaks corresponding to the semicircles of BGCE and $NiS/CoS/NiCo_2S_4$/GCE has shifted. The peaks around the frequency range of 10^3 Hz for BGCE and $NiS/CoS/NiCo_2S_4$/GCE are all attributed to the bulk electron transfer resistance [20]. Last but not the least, the Z_r–$\omega^{-1/2}$ (angular frequency $\omega=2\pi f$) curves in the low frequency region (below 1.0 Hz) is displayed in Fig. 3f. Apparently, the slope of $NiS/CoS/NiCo_2S_4$/GCE is slightly larger than that of BGCE, that is to say, the diffusion resistance of the glucose into the $NiS/CoS/NiCo_2S_4$ body is high. This may be caused by the space structure of glucose.

4. Conclusions

In a word, $NiS/CoS/NiCo_2S_4$ hierarchical structure is fabricated by hydrothermal method. The supercapacitive and glucose sensing performance have been investigated. It reveals high specific capacitance and excellent glucose sensing behavior. The redox reaction of glucose on the $NiS/CoS/NiCo_2S_4$ is controlled by the diffusion process of glucose from the solution to the electrode surface. These results maybe lay the foundation for the nickel and cobalt based electrode materials.

Acknowledgement

This work is financially supported by the Youth Backbone Teacher Project of Henan University of Technology (No.2015007) and the Institutions of Higher Learning Key Scientific Research Project (No.19B150005).

References

[1] F.Y. Zhou, Q.L. Liu, J.J. Gu, W. Zhang, D. Zhang, J. Power Sources 273 (2015) 945.

[2] X.B. Xu, W. Zhong, X. Zhang, J. Dou, Z.G. Xiong, Y. Sun, T.T. Wang, Y.W. Du, J. Colloid Interf. Sci. 543 (2019) 147.

[3] S. Rafai, C. Qiao, M. Naveed, Z.T. Wang, W. Younas, S. Khalid, C.B. Cao, Chem. Eng. J. 362 (2019) 576.

[4] W. Abbas, N. Akhtar, Q.L. Liu, T.F. Li, I. Zada, L.L. Yao, R. Naz, W. Zhang, M. Ehsan Mazhar, D. Zhang, D.L. Ma, J.J. Gu, Sens. Actuators B 282 (2019) 617.

[5] H. Mao, Z.Q. Cao, X. Guo, D.Y. Sun, D.L. Liu, S.Y. Wu, Y. Zhang, X.M. Song, ACS Appl. Mater. Interfaces 11 (2019) 10153.

[6] V. Sridhara, H. Park, J. Alloy. Compd. 764 (2018) 490.

[7] Z.Y. Yang, X.H. Zheng, J.B. Zheng, Sens. Actuators B 253 (2017) 34.

[8] L.F. Shen, L. Yu, H.B. Wu, X.Y. Yu, X.G. Zhang, X.W. (David) Lou, Nat. Commun. 6 (2015) 6694.

[9] R. Naz, M. Imtiaz, Q.L. Liu, L.L. Yao, W. Abbas, T.F. Li, I. Zada, Y. Yuan, W.S. Chen, J.J. Gu, Carbon 152 (2019) 697.

[10] P.K. Kannan, C.X. Hu, H. Morgan, C.S. Rout, Chem. Asian J. 11 (2016) 1837.

[11] D.L. Chen, H.Y. Wang, M.H. Yang, Anal. Methods 9 (2017) 4718.

[12] M. Lu, N. Gao, X.J. Zhang, G.S. Wang, RSC Adv. 9 (2019) 5550.

[13] C.Q. Feng, Y.R. Li, M. Wang, G.Y. Zhao, Z.S. Wang, Electrochim. Acta 301 (2019) 220.

[14] C.Q. Duan, Y.H. Dong, Q.L. Sheng, J.B. Zheng, Talanta 198 (2019) 23.

[15] A. Somdee, J. Alloy. Compd. 777 (2019) 1251.

[16] N. Wang, Q.L. Liu, D.M. Kang, J.J. Gu, W. Zhang, D. Zhang, ACS Appl. Mater. Interfaces 8 (2016) 16035.

[17] F.Y. Zhou, Q.L. Liu, J.J. Gu, W. Zhang, D. Zhang, Electrochim. Acta 170 (2015) 328.

[18] M. Rezaeinasab, A. Benvidi, M.D. Tezerjani, S. Jahanbani, A.H. Kianfar, M. Sedighipoor, Electroanal. 29 (2017) 423.

[19] K. Liu, J.L. Cui, J.P. Yin, J.Z. Man, Y.F. Cui, Z.S. Wen, J.C. Sun, J. Alloy. Compd. 765 (2018) 229.

[20] J. Liu, Q. Zhang, T. Zhang, J.T. Li, L. Huang, S.G. Sun, Adv. Funct. Mater. 25 (2015) 3599.

Conflict of interest statement

The authors declare that we have no financial and personal relationships with other people or organizations that can inappropriately influence this work.

Signature: Yuandong Xu (Corresponding Author)

Date: Sep. 11, 2019

Graphical Abstract

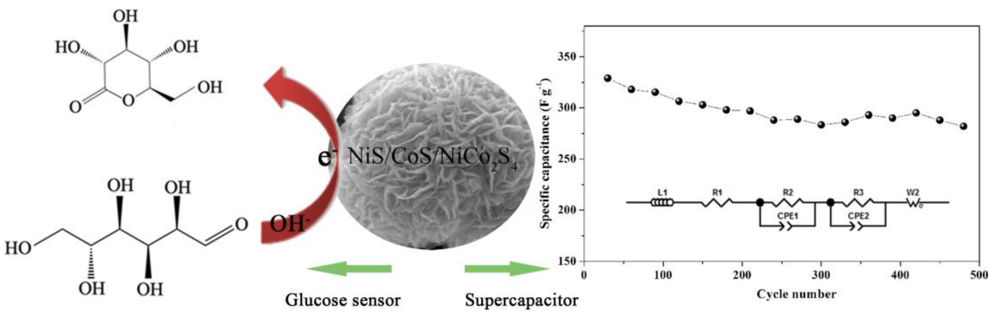

Highlights

- $NiS/CoS/NiCo_2S_4$ microflower is prepared via hydrothermal method.
- $NiS/CoS/NiCo_2S_4$ displays favorable pseudocapacitive and glucose sensing behavior.
- The redox reaction of glucose on $NiS/CoS/NiCo_2S_4$ is controlled by the diffusion process.